Journal of Magnetic Resonance **142,** 372–378 (2000)
doi:10.1006/jmre.1999.1945, available online at http://www.idealibrary.com on IDEAL®

Low-Frequency Molecular Dynamics Studied by Spin-Lock Field Cycling Imaging

E. Anoardo,* C. Hauser,† and R. Kimmich†

*Facultad de Matemática, Astronomía y Física, Universidad Nacional de Córdoba, Ciudad Universitaria, 5000 Córdoba, Argentina; and †Sektion Kernresonanzspektroskopie, Universität Ulm, 89069 Ulm, Germany

Received September 9, 1998; revised August 26, 1999

Spin-lock adiabatic field cycling imaging (SLOAFI) relaxometry was shown to be a useful technique for obtaining a fast study of spin–lattice relaxation dispersion in the rotating frame. The aim of the present article is to describe some technical aspects of the experiment in more detail, while showing simple examples that can be compared with laboratory frame relaxation. We also present here a general discussion of the equations for an off-resonance experiment used to analyze low-frequency molecular dynamics. © 2000 Academic Press

Key Words: **off-resonance spin–lattice relaxation; relaxometry; low-frequency molecular dynamics; adiabatic fast switching of magnetic field gradients; imaging.**

1. INTRODUCTION

Spin-lock adiabatic field cycling imaging (SLOAFI) relaxometry was described in a previous paper. The technique was applied to polydimethylsiloxane (PDMS 68000) at 293 K (*1*). In that work it was concluded that the method could be useful for a fast inquiry about low-frequency spin–lattice relaxation. In this new paper, the effective rotating frame spin–lattice relaxation time is expressed in terms of the involved spectral densities, but carefully keeping the effective frequency dependence of its coefficients. Equations of this new paper are derived from an expression equivalent to Eq. [10] from Ref. (*1*). However, in that work, the frequency dependence of the spectral densities coefficients was not emphasized. This is a very important task to consider, mainly because this case is different to other common NMR relaxation parameters such as T_1, T_{1D}, T_2, T_{1Q}, and $T_{1\rho}$, where coefficients are not frequency dependent.

In order to have a better understanding of this experiment we made some new measurements using well-known examples: a first case where the involved spectral densities are nearly frequency independent (slightly doped water) and a second example where the laboratory frame relaxation is dominated by a one-correlation time isotropic molecular movement (pivalic acid). In this article we also discuss how to handle the information provided by the experiment and the low-frequency spectral densities. Is worth mentioning that the dynamical information of the molecular system is contained in the spectral densities and not on the frequency dependence of the measured effective relaxation time itself. Results obtained in doped water are a clear example of this last statement: even when spectral densities are treated as frequency independent, the relaxation curve shows an important dispersion at low frequencies.

We start the analysis by discussing the adequate equation for off-resonance relaxation in the rotating frame. The aim of the work is to get the dynamical information of the system in such a way that it can be easily compared with that extracted from fast-field cycling laboratory frame spin–lattice relaxation dispersion ($T_1(\omega_0)$). This comparison could be important in order to inquire about the low-frequency properties of laboratory and rotating frame spin–lattice relaxation.

The adiabatic switching characteristics for the power magnetic field gradients were also improved in this new experiment, allowing us to extend the relaxation curves to higher frequencies. Details are described in Section 3.

2. EQUATION FOR OFF-RESONANCE SPIN–LATTICE RELAXATION

Spin–lattice relaxation at low Larmor frequencies has been studied in a different context from the early years of nuclear magnetic resonance (NMR). Both weak and strong collision limits were considered in several works with the principal aim of studying slow molecular motions. In a NMR spin–lattice relaxation experiment of any kind, the dynamical information is contained in spectral density functions. Depending on the technique used, the experiment could be simultaneously sensitive to more than one time scale. Therefore, the art of designing a relaxation experiment resides (in part) in the ability of the experimenter to get the dynamical spectral information of interest in a reliable and controlled way. In fact, this is the critical point for laboratory frame field cycling relaxation experiments at low fields: the presence of the earth field and dipolar local fields, the shape and time of the switching magnetic field, etc., become extremely important parameters of the experiment that are usually hardly considered in the theory later. On the other hand, rotating frame relaxation techniques

1090-7807/00 $35.00

are not exempt from this observation; the parameters mentioned can influence results in a different way and/or other parameters could be more important while absent in a laboratory frame experiment (and vice versa). The principal goal of the present work was to check, using very simple and known examples, how to contrast the low-frequency rotating frame spectral density with equivalent information obtained using laboratory frame field cycling NMR.

2.1. Resonantly Rotating Frame Relaxation

Since Redfield's first considerations about the properties of resonantly rotating magnetic field (B_1) (*2*), several authors have considered the properties of spin–lattice relaxation along this field. Using first-order perturbation theory and assuming spin temperature, Look and Lowe treated the case for a system of $I = \frac{1}{2}$ interacting spins undergoing random internal motion described in terms of one correlation time in the weak collision limit (*3*). A more general equation for the weak collision limit was obtained by Kelly and Sholl using the density operator assuming stochastic time dependence for the lattice variables (*4*):

$$\frac{1}{T_{1\rho}(\omega_1,\omega_0)} = \frac{K}{4}\left[J_0(2\omega_1) + 10J_1(\omega_0) + J_2(2\omega_0)\right], \qquad [1]$$

where $K = \frac{3}{2}\gamma^4\hbar^2 I(I+1)$, $\omega_1 = \gamma B_1$ and $\omega_0 = \gamma B_0$, γ being the magnetogiric ratio of the nuclei, B_0 the Zeeman static (laboratory frame) magnetic field, and J_0, J_1, and J_2 the corresponding spectral densities. A simple observation of this last equation tells us that $T_{1\rho}$ is sensitive to two different time scales: ω_1 and ω_0. In consequence, if the experiment is carried out in a constant Zeeman magnetic field, i.e., fixed ω_0, the two last terms of the equation will be constants. In general, J_1 and J_2 can be evaluated from a T_1 experiment or a combination of T_1 and T_{1D} (Jeener–Broekaert) experiments at the same Zeeman field value. The equation then suggest that $J_0(2\omega_1)$ can be obtained by repeating the experiment for different B_1 amplitudes. In this case, the ω_1 frequency band will run from a minimum value depending on the minimum possible B_1 allowing a spin-locked ordered state to a maximum value depending on the output power of the transmitter and the quality of the probe. Using high power makes the experiment difficult because of several reasons, such as dielectric rupture in the capacitors of the tuning circuit and heating of the sample coil. This is reflected in a high frequency limit for the resonantly rotating frame study of few tens of KiloHertz for protons ($\omega_1/2\pi$).

2.2. Off-Resonance Rotating Frame Relaxation

The simpler way to avoid high power in the transmission can be achieved by using the off-resonance condition. In this case, the magnetization can be locked along the effective field $B_{\text{eff}} = \sqrt{B_1^2 + (B_0 - \omega_{\text{RF}}/\gamma)^2}$ (with ω_{RF} being the radiofrequency (RF) angular frequency) in the rotating frame, thus now the covered frequency interval will depend on this field ($\omega_{\text{eff}} = \gamma B_{\text{eff}}$). This condition can be obtained in two ways: using off-resonant radio frequency fields or by changing the Zeeman field during the spin-lock.

The general case for off-resonance relaxation in the weak collision limit was successfully treated by Jones (rigorously for spin $\frac{1}{2}$) (*5*) and was also considered and used by several authors for different purposes (*6–11*). When the relation $\omega_0 \gg \omega_{\text{eff}}$ holds for the whole effective frequency interval, the general equation of Jones describing the spin–lattice relaxation in the effective field can be rewritten as

$$\frac{1}{T_{1\rho}^{\text{eff}}} = \frac{K}{4}\left\{aJ_0(\omega_{\text{eff}}) + bJ_0(2\omega_{\text{eff}}) + cJ_1(\omega_0) + dJ_2(2\omega_0)\right\}, \qquad [2]$$

where the coefficients of the spectral densities are given by

$$a = \sin^2\theta\cos^2\theta$$

$$b = \sin^4\theta$$

$$c = 4\left[\cos^2\left(\frac{3\theta}{2}\right)\cos^2\left(\frac{\theta}{2}\right) + \sin^2\left(\frac{3\theta}{2}\right)\sin^2\left(\frac{\theta}{2}\right) + 4\sin^2\theta\cos^4\left(\frac{\theta}{2}\right) + 4\sin^2\theta\sin^4\left(\frac{\theta}{2}\right)\right]$$

$$d = \sin^2\theta\left[\cos^4\left(\frac{\theta}{2}\right) + \sin^4\left(\frac{\theta}{2}\right)\right] + 4\left[\cos^8\left(\frac{\theta}{2}\right) + \sin^8\left(\frac{\theta}{2}\right)\right],$$

with $\theta = \arctan(\omega_1/(\omega_0 - \omega_{\text{RF}}))$ and $\omega_{\text{eff}} = \sqrt{(\omega_0 - \omega_{\text{RF}})^2 + \omega_1^2}$. After reducing the coefficients, the previous equation can be written in terms of $T_1(\omega_0)$:

$$\frac{1}{T_{1\rho}^{\text{eff}}(\omega_{\text{eff}},\omega_0)} = \frac{1}{T_1(\omega_0)}\left(1 + \frac{3}{2}\sin^2\theta\right) - \frac{9}{4}K\sin^2\theta J_2(2\omega_0) + \frac{K}{4}\sin^2\theta(\sin^2\theta J_0(2\omega_{\text{eff}}) + \cos^2\theta J_0(\omega_{\text{eff}})), \qquad [3]$$

where

$$\frac{1}{T_1(\omega_0)} = K[J_1(\omega_0) + J_2(\omega_0)]. \qquad [4]$$

It can be observed that if $\theta = \pi/2$ (on resonance condition) Eqs. [2] and [3] become equal to Eq. [1]. It is also worth mentioning that in case of extreme off-resonance condition

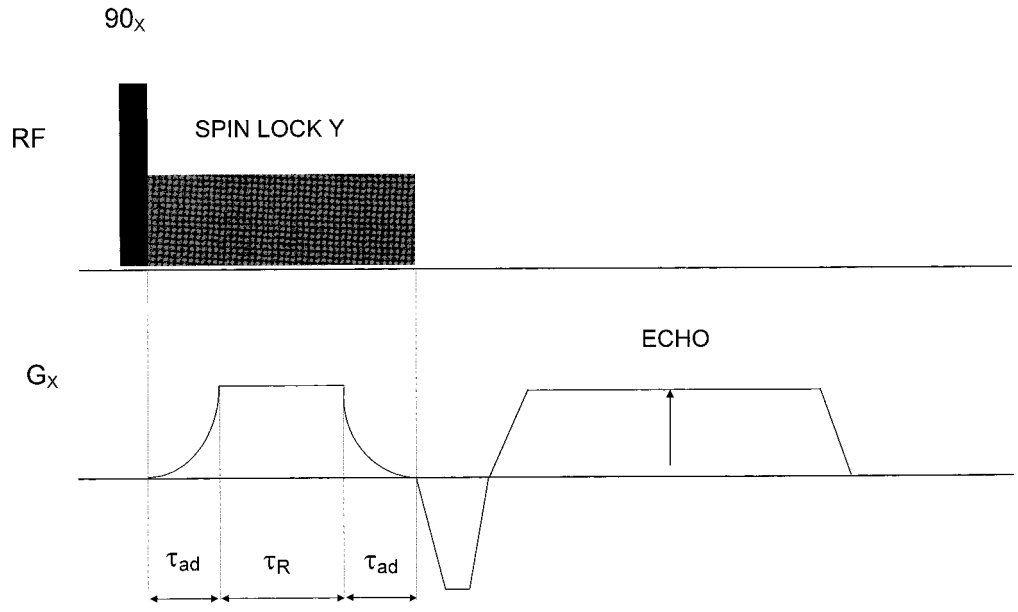

FIG. 1. Pulse sequence of SLOAFI experiment. The magnetization is spin-locked while a magnetic field gradient G_x is adiabatically switched on to produce a spatial distribution of the effective Larmor frequency along the sample. This condition is held during a relaxation period where the locked magnetization relaxes at the corresponding effective frequency depending on the position. At the end of the interval the gradient is adiabatically switched off and the remaining magnetization is refocused along the spin-lock field. Finally, the partially relaxed magnetization is imaged using the gradient echo sequence. The experiment is repeated for different relaxation intervals τ_R to obtain the temporal evolution of the profiles.

($\theta \approx 0$), $T_{1\rho}^{\text{eff}}(\omega_{\text{eff}}, \omega_0)$ approaches $T_1(\omega_0)$. Notice the important difference between the previous equation with respect to T_1 or $T_{1\rho}$ equations: in this general case, the coefficients of spectral densities are also frequency dependent. This is an important point to be considered when analyzing off-resonance profiles. The above equation suggests that an off-resonance experiment will be convenient in order to increase the effective frequency window since ω_{eff} can be set at least one order of magnitude larger than $2\omega_1$. The technique can be exploited by shifting the RF frequency during the spin-lock (*8, 10*) or by changing the value of the Zeeman field for fixed RF frequency (*5*). In both cases the $T_{1\rho}^{\text{eff}}(\omega_{\text{eff}})$ dispersion is obtained point by point repeating the measurement sequence at different off-resonance conditions. By combining magnetic field gradients (B_0 or B_1) and one-dimensional imaging it is possible to obtain a fast $T_{1\rho}^{\text{eff}}(\omega_{\text{eff}})$ dispersion in a broad frequency band in a single experiment. This is the main advantage of the SLOAFI sequence.

3. EXPERIMENTAL DETAILS

3.1. Implementing SLOAFI

Figure 1 shows the typical pulse sequence for a laboratory frame (B_0 gradient) SLOAFI experiment. The technique consists of a spin-lock of the magnetization while adiabatically switching a B_0 gradient in order to produce an off-resonance relaxation along the sample. The field gradient causes a spatial distribution of the effective Larmor frequency along the gradient direction. Therefore, the locked magnetization in a given position relaxes during the time interval τ_R at the corresponding effective frequency of that position. At the end of the relaxation interval τ_R, the B_0 gradient is adiabatically switched off in order to get back the whole remaining magnetization along the spin-lock field (B_1). The partially relaxed magnetization is finally imaged by acquiring the gradient echo. The experiment is repeated for different values of the relaxation interval τ_R.

The switching of the magnetic field gradient should be done in an adiabatic way in order to preserve the spin polarization. This means that no transitions must occur between the populations during the process. From the experimental point of view, the loss of magnetization during the switching time should be kept as small as possible (in the best case, it could be undetectable within experimental resolution). The general conditions for obtaining an adiabatic B_0 gradient switching were discussed in a previous paper (*1*).

The obtained result for the off set frequency $\Omega = \omega_0 - \omega_{\text{RF}}$ with respect to the on-resonance frequency ω_1 during the switching time t was

$$\Omega(t) = \frac{c\omega_1 t}{\sqrt{1 - (c\omega_1 t)^2}}, \qquad [5]$$

where c is a constant much smaller than 1. From the theoretical point of view, this equation means that the gradient should be increased very slowly at the beginning while rising faster as the

off-resonance angles decrease. Notice that a very fast rise of the gradient magnitude could be necessary for a strong gradient, which in turn becomes highly desirable in order to get a broad off-resonance frequency band. In this case, the very fast increasing current on the gradient coils and the abrupt change on this value produced while switching off after reaching the maximum value will produce an undesirable strong mechanical stress in the coils. In the new measurements we used a truncated sinc function instead of the theoretically calculated shape, obtaining a better overall performance: we eliminated the strong mechanical stress in the gradient coils and we even got a shorter switching time while keeping the adiabatic condition. This could be an important experimental observation because in general sequence editor software contains sinc functions in the library. We could successfully reduce the adiabatic switching time τ_{ad} from an initial value of 5 ms for 100 mT/m gradient (with strong stress in the coils) to a value of only 1.2 ms for a 140 mT/m gradient.

3.2. Data Handling in a SLOAFI Experiment

In the following discussion we describe the evolution of the magnetization in a SLOAFI experiment and how we processed data in order to obtain the $T_{1\rho}^{\text{eff}}$ dispersion curve. The evolution of the magnetization in the rotating frame for a given off resonance angle is given by (*12*)

$$M_{\rho}^{\text{eff}}(t) = (M_0 - M_{\rho 0}^{\text{eff}})\exp(-t/T_{1\rho}^{\text{eff}}) + M_{\rho 0}^{\text{eff}}, \qquad [6]$$

where $M_0 = M_{\rho}^{\text{eff}}(0)$ is the initial spin-locked magnetization. In the previous equation the off-resonance equilibrium magnetization $M_{\rho 0}^{\text{eff}}$ is given by

$$M_{\rho 0}^{\text{eff}}(\omega_{\text{eff}}) = M_0 \frac{T_{1\rho}^{\text{eff}}(\omega_{\text{eff}})}{T_1(\omega_0)} \cos\theta, \qquad [7]$$

where

$$\cos\theta = \frac{\omega_0 - \omega_{\text{RF}}}{\omega_{\text{eff}}}. \qquad [8]$$

Notice that on-resonance $\theta = \pi/2$ and therefore $M_{\rho 0}^{\text{eff}} = 0$. This condition should be held at all times in the position of the sample where the magnetic field gradient is zero. From this position to one side of the sample corresponds a positive gradient offset, while for the other side the contrary holds. This means that the magnetization across one half of the sample relaxes according to an *inversion recovery* (when $\theta > \pi/2$), while the other half just evolves from the initial value M_0 to the equilibrium value $M_{\rho 0}^{\text{eff}}$ (the final value in both cases). Figure 2 shows a *waterfall* plot of the profile evolution for different τ_R obtained using the SLOAFI pulse sequence in a sample of water slightly doped with copper sulfate. For this example, the zero point of the magnetic field gradient is approximately in the geometric center of the sample. It can be clearly seen that the right part of the profile evolves taking the mentioned inversion recovery (in modulus), while the left part evolves to the final equilibrium value. For cases where $M_{\rho 0}^{\text{eff}} \simeq M_0$ the left side of the profile is relaxing exponentially from a starting value which is very close to the final equilibrium value. As a consequence, it is not convenient to calculate the relaxation time from exponential fitting. Therefore, inversion recovery curve fitting becomes adequate for evaluating the relaxation times. This fact suggest that the frequency window can be enlarged by locating the zero gradient point at one extreme of the sample.

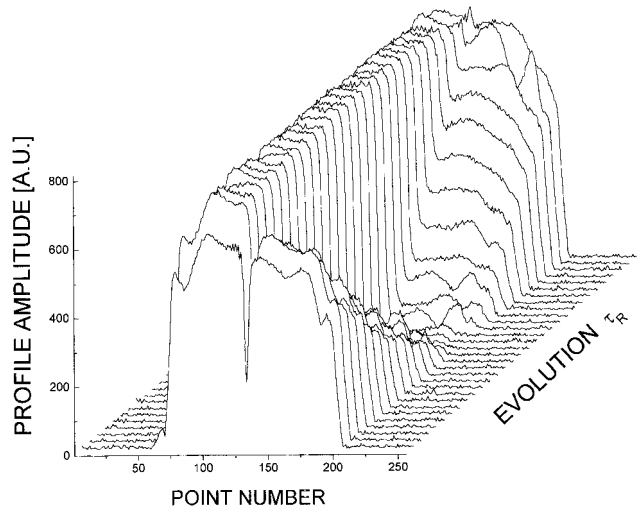

FIG. 2. Temporal evolution of the profiles with the relaxation time interval τ_R in a sample of doped water. The different evolution at each side of the zero magnetic field gradient point located approximately at the center of the sample can be easily observed.

Each point of the point number axis in Fig. 2 corresponds to a defined off-resonance frequency value. The evolution of the magnetization corresponding to a given point number in the right side of the profile is displayed in Fig. 3. The evolution curve was fitted using the modulus of Eq. [6]. From the fitting of the different inversion recovery curves, a $T_{1\rho}^{\text{eff}}$ value can be calculated for each point of the profile, i.e., for each effective frequency. In order to assign a particular off-resonance frequency to a given point in the profile we can start from the following expression:

$$\omega_{\text{eff}}(x) = \sqrt{[\omega_0(x) - \omega_{\text{RF}}]^2 + \omega_1^2}, \qquad [9]$$

where x is the position along the sample and

$$\omega_0(x) = \gamma(B_0 + G_x x). \qquad [10]$$

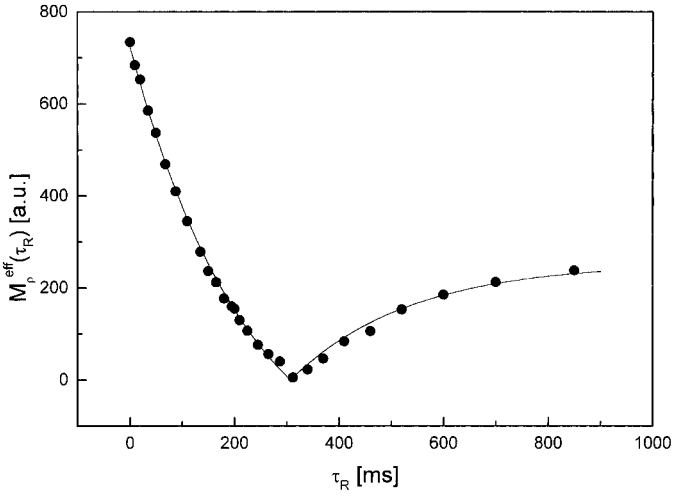

FIG. 3. Magnetization relaxation curve for a definite effective frequency corresponding to the "inversion recovery" evolution.

If $\omega_{RF} = \gamma B_0$ we obtain

$$\omega_{eff}(x) = \sqrt{\omega_1^2 + (\gamma G_x x)^2}. \quad [11]$$

Because each point of the profile corresponds to a particular position x along the sample, from this last expression the correspondence between the position in the profile and the off-resonance frequency can be easily seen. It can be observed that both sides of the profile will have the same frequency assignment starting from the zero gradient point. As can be seen from Eq. [11] it is highly desirable to have the spin-lock amplitude (ω_1) as low as possible while using the magnetic field gradient as strong as possible, in order to cover a broad frequency range in the experiment. Is important to notice that the linearity of the magnetic field gradient is only a matter of convenience when doing data evaluation. In some experiments it could be very important to extend the measurements to higher frequencies. In these cases, very strong gradients must be used without being able to keep the linearity anymore. This fact does not limit the use of the technique, being only necessary to record the spatial dependence of the field gradient across the sample for correction.

4. TEST EXPERIMENTS

In order to test Eq. [3] we run SLOAFI in very simple cases. Measurements were done in a 5-T homebuilt NMR tomograph using a Bruker microimaging probehead with an 11-mm-diameter solenoidal sample coil.

4.1. SLOAFI in Doped Water

This can be considered the simplest case because the spectral densities are nearly frequency independent at low Larmor frequencies (as can be easily checked using a T_1 field cycling experiment). Of course for higher concentrations of dopants, a low-frequency dispersion could be present in the relaxation due to the paramagnetic impurities. Assuming that this effect is negligible, Eq. [3] becomes

$$\frac{1}{T_{1\rho}^{eff}} = \frac{1}{T_1}\left[1 + \frac{3}{2}\left(\frac{\omega_1}{\omega_{eff}}\right)^2\right] - (A - B)\left(\frac{\omega_1}{\omega_{eff}}\right)^2, \quad [12]$$

where $A = (9/4)KJ_2$ and $B = (K/4)J_0$. In this approximation we assume

- $J_2 = J_2(\omega_0)$ is a constant because the experiment is done at a fixed external magnetic field.
- We assume that the spectral densities are frequency independent and in consequence $J_0 = J_0(\omega_e)$ should be also considered a constant.
- For the same reason we assume that $J_0(\omega_e) = J_0(2\omega_e)$.

Figure 4 contains experimental data and the fitting obtained using Eq. [12]. The values of $T_1 = 254{,}45$ ms and $A - B = 0.00572$ ms^{-1} were obtained from the fitting process. The T_1 obtained from fitting perfectly matches the experimental value measured by a conventional two $\pi/2$ pulses (255 ms). Taking into account the factors of the spectral densities 6:4 between J_0 and J_2 for complete isotropic dipolar interaction, the ratio between A and B should be 6:1. From this observation is possible to obtain the numeric values of J_0 and J_2 (the ratio 6:1 could be different in the presence of other kind of relaxation mechanism, e.g., scalar coupling (*6*). The important point to observe in this example is that spectral densities are frequency independent and not $T_{1\rho}^{eff}$ itself. In fact, as was previously

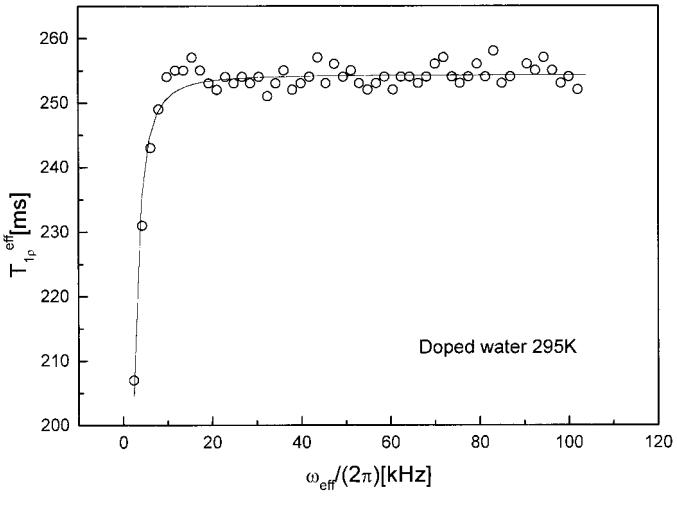

FIG. 4. $T_{1\rho}^{eff}$ (ω_{eff}) dispersion profile for water. The solid line corresponds to the fitting using Eq. [12]. Experimental error of relaxation times is less than 4%, even when the noise in the profiles is over 10%. This can be attributed in part to the nature of the magnetization evolution curves (Fig. 3). The minimum point amplitude reached by the magnetization due to the "inversion recovery" character provides an unambiguous constraint for the fitting process.

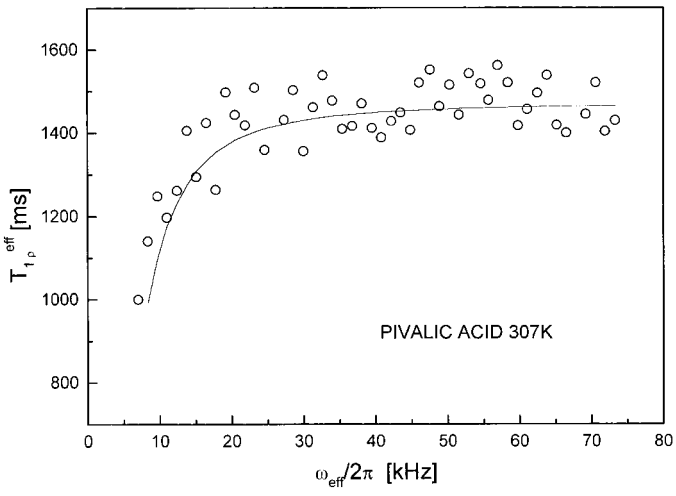

FIG. 5. Dispersion profile for pivalic acid at 307 K in the plastic phase. Solid line represents the obtained fitting using Eq. [13]. Now experimental errors are less than 15%.

pointed in the text, this is a direct consequence of the frequency-dependent coefficients of the spectral densities.

4.2. SLOAFI in Pivalic Acid

As a second well-known test substance we used pivalic acid in the plastic phase at 307 K. It is known that in this phase the compound has a low frequency relaxation characterized by a definite correlation time $\tau_c \simeq 10^{-3}$ ms (*13*). Therefore, in this case we fitted data using the typical isotropic motions Lorentzian spectral densities for $J_0(\omega_{\text{eff}})$ and $J_0(2\omega_{\text{eff}})$. On the other hand, $J_2(\omega_0)$ is a fixed value which was evaluated from the T_1 value. In fact, assuming complete isotropic relaxation mechanisms at ω_0, the relation $J_2(\omega_0) = 4J_1(\omega_0)$ holds (*14*). Equation [3] can be written as

$$\frac{1}{T_{1\rho}^{\text{eff}}} = \frac{1}{T_1}\left(1 + \frac{3}{2}z\right) - Az + Bz[zJ_0(\omega_{\text{eff}}) + (1-z)J_0(2\omega_{\text{eff}})], \qquad [13]$$

where A has the same meaning as the previous case, $B = K/4$, $z = (\omega_1/\omega_{\text{eff}})^2$, and

$$J_0(\omega_{\text{eff}}) = \frac{\alpha\tau_c}{1 + (\omega_{\text{eff}}\tau_c)^2}, \qquad [14]$$

with α being the spectral density amplitude.

Figure 5 shows experimental data and a fitting curve using Eq. [13]. Notice that if $J_2(\omega_0) = 4J_1(\omega_0)$ the constant A becomes equal to $9/(5T_1) = 1.22 \cdot 10^{-3}$ ms^{-1}. The fitting process was done using as input parameters the measured value of $T_1 = 1470$ ms and $A = 1.22 \cdot 10^{-3}$ ms^{-1} (calculated according to the previous observation). The values of $B\alpha = 3$ ms^{-2} and $\tau_c = 10^{-3}$ ms were obtained from the fitting process. It can be observed that the term containing $J_2(\omega_0)$ has an insignificant weight in the fitting, in correspondence with the fact that $\omega_0\tau_c \gg 1$. The obtained value for the correlation time is in agreement with determinations from other authors (*13*).

5. CONCLUSIONS

We described experimental details of SLOAFI relaxometry and applied the technique in two simple cases. Results indicates that there exists a close correspondence between the rotating frame and the low field laboratory frame spectral densities. However, this result may not be extended for all samples, especially those with high magnetic anisotropy.

New technical details were discussed and the time needed to switch adiabatically to an off-resonance condition was considerably improved by using an easy available pulse shape. This has an important advantage when dealing with short relaxation times in the sense that relaxation during the transit interval τ_{ad} becomes less important. In the opposite limit, i.e., when the off-resonance relaxation time is long, it is worthwhile to consider possible effects due to self-diffusion under the application of strong magnetic field gradients. The only way this could affect the results is that the molecule diffuses during τ_R to a sufficiently different ω_{eff}. The consequence would be a sort of smearing out effect on the $T_{1\rho}^{\text{eff}}$ dispersion. However, the length scale on which the effective field varies sufficiently in this sense is relatively long. It is hard to imagine that the relaxation time changes significantly within experimental errors on a typical RMS distance of few micrometers during τ_R.

Application of SLOAFI on samples with short T_2 (spin–spin relaxation) becomes complicated because very strong gradients are necessary for a fast refocusing of the magnetization. This case was tested in thermotropic mesogens. Special care must be taken when using SLOAFI in samples with magnetic dopants such as ferrofluids, ferronematics, and all doped low-viscosity mesogens. In these cases the magnetic particles can diffuse in the sample during τ_R because the presence of the strong magnetic field gradient.

Another important application of the experiment is for studying cross relaxation. In this way we ran measurements in deuterated gelatins to study the rotating frame proton–deuteron quadrupolar dips (*15*). However, this experiment requires a more detailed treatment and we prefer to leave it for a rear consideration.

ACKNOWLEDGMENTS

The authors thank Dipl. A. Klem for his kind collaboration during the setup of the experiment. E.A. thanks the Deutscher Akademischer Austauschdienst (DAAD) for economic support during the period of work in Germany.

REFERENCES

1. R. Kimmich, J. Barenz, and J. Weis, *J. Magn. Reson. A* **117,** 228 (1995).

2. A. G. Redfield, *Phys. Rev.* **98,** 1787 (1955).
3. D. C. Look and I. J. Lowe, *J. Chem. Phys.* **44,** 2995 (1966).
4. S. W. Kelly and C. A. Sholl, *J. Phys. Condens. Matter* **4,** 3317 (1992).
5. G. P. Jones, *Phys. Rev.* **148,** 332 (1966).
6. J. S. Blicharski, *Acta Phys. Polonica A* **41,** 223 (1972).
7. J. F. Jacquinot and M. Goldman, *Phys. Rev. B* **8,** 1944 (1973).
8. B. A. Cornell and J. M. Pope, *J. Magn. Reson.* **16,** 172 (1974).
9. T. K. Leipert, J. H. Noggle, W. J. Freeman, and D. L. Dalrymple, *J. Magn. Reson.* **19,** 208 (1975).
10. T. L. James, G. B. Matson, I. D. Kuntz, R. W. Fisher, and D. Buttlaire, *J. Magn. Reson.* **28,** 417 (1977).
11. T. L. James and G. Matson, *J. Magn. Reson.* **33,** 345 (1979).
12. R. Kimmich, "NMR Tomography Diffusometry Relaxometry," Springer Verlag, Berlin (1997).
13. S. G. Stapf, personal communication.
14. A. Abragam, "The Principles of Nuclear Magnetism," Clarendon Press, Oxford (1961).
15. E. Anoardo and R. Kimmich, "Symposium on Field-Cycling NMR Relaxometry: Techniques, Applications, Theories," Berlin (1998).